

Article

Dynamic Repositioning of Aerial Base Stations for Enhanced User Experience in 5G and Beyond

Shams Ur Rahman ¹, Ajmal Khan ², Muhammad Usman ¹, Muhammad Bilal ³, You-Ze Cho ^{4,*}
and Hesham El-Sayed ⁵

- ¹ Department of Computer Science, UET Mardan, Charsadda Road, Mardan 23200, Pakistan; shams@uetmardan.edu.pk (S.U.R.); usman@uetmardan.edu.pk (M.U.)
- ² Department of Artificial Intelligence and Big Data, Woosong University, 171 Dongdaejon-ro, Dong-gu, Daejeon 34606, Republic of Korea; engajmal@wsu.ac.kr
- ³ Department of Computer Engineering, Hankuk University of Foreign Studies, Yongin-si 17035, Republic of Korea; m.bilal@ieee.org
- ⁴ School of Electronics and Electrical Engineering, Kyungpook National University, Daegu 41566, Republic of Korea
- ⁵ Computer and Network Engineering Department, College of Information Technology, United Arab Emirates University, Al Ain 16427, United Arab Emirates; helsayed@uaeu.ac.ae
- * Correspondence: yzcho@ee.knu.ac.kr

Abstract: The ultra-dense deployment (UDD) of small cells in 5G and beyond to enhance capacity and data rate is promising, but since user densities continually change, the static deployment of small cells can lead to wastes of capital, the underutilization of resources, and user dissatisfaction. This work proposes the use of Aerial Base Stations (ABSs) wherein small cells are mounted on Unmanned Aerial Vehicles (UAVs), which can be deployed to a set of candidate locations. Furthermore, based on the current user densities, this work studies the optimal placement of the ABSs, at a subset of potential candidate positions, to maximize the total received power and signal-to-interference ratio. The problems of the optimal placement for increasing received power and signal-to-interference ratio are formulated, and optimal placement solutions are designed. The proposed solutions compute the optimal candidate locations for the ABSs based on the current user densities. When the user densities change significantly, the proposed solutions can be re-executed to re-compute the optimal candidate locations for the ABSs, and hence the ABSs can be moved to their new candidate locations. Simulation results show that a 22% or more increase in the total received power can be achieved through the optimal placement of the Aerial BSs and that more than 60% users have more than 80% chance to have their individual received power increased.

Keywords: 5G; dynamic repositioning; ultra-dense deployment; UAV network; throughput maximization; optimal positioning



Citation: Rahman, S.U.; Khan, A.; Usman, M.; Bilal, M.; Cho, Y.-Z.; El-Sayed, H. Dynamic Repositioning of Aerial Base Stations for Enhanced User Experience in 5G and Beyond. *Sensors* **2023**, *23*, 7098. <https://doi.org/10.3390/s23167098>

Academic Editors: Khaled Rabie, Pascal Lorenz, Muhammad Asghar Khan, Syed Agha Hassnain Mohsan and Muhammad Shafiq

Received: 17 June 2023

Revised: 1 August 2023

Accepted: 7 August 2023

Published: 11 August 2023



Copyright: © 2023 by the authors. Licensee MDPI, Basel, Switzerland. This article is an open access article distributed under the terms and conditions of the Creative Commons Attribution (CC BY) license (<https://creativecommons.org/licenses/by/4.0/>).

1. Introduction

5G networks and beyond face the enormous challenge of satisfying the ever-increasing demand for more user capacity, higher data rates, and lower latency. These demands are fueled by the proliferation of increasingly data-hungry smart devices and applications such as augmented reality, virtual reality, and 3D multimedia. Ericsson Mobility Report 2022 [1] projections show that by the end of 2022, monthly average usage per smartphone will surpass 15 GB, and by 2027, 5G subscriptions will reach 4.4 billion. Moreover, according to the report, traffic has grown by more than 15 times in the past 5 years (as of June 2022), and the total mobile traffic will surge to 328 Exabytes per month in 2028, which will be a 5× increase compared to 2022. According to the report, 5G will be the main driver for fueling these demands. To meet such demands, 5G aims to bring about a 100× increase in capacity and a 1000× increase in user data rates compared to 4G [2]. To achieve these ambitious

targets, a variety of advanced techniques are being employed, including massive MIMO (Multiple-Input, Multiple-Output), millimeter Wave, and ultra-dense deployment (UDD) of small cells [2].

UDD involves the deployment of many closely spaced base stations which incurs tremendous capital expenditure (CAPEX) and operational expenditure (OPEX); therefore, it is important to maximize the utilization of UDD resources. However, due to user mobility and activities, user density changes all the time [3]. For example, user density around shopping areas is higher on weekends and in the evening compared to weekdays and work hours, respectively; in the evening time, user density around parks is higher compared to work hours; during sports events, density around sports venues is drastically higher; and during rallies and protests, user density constantly changes. Such fluctuations in user density result in some parts of the network being overloaded, whereas other parts are under-utilized if the deployment is fixed. Therefore, it is highly desirable, on the part of service providers, to be able to adjust the deployment, i.e., location, of small cells according to user density, which can be achieved by mounting the small cells onto unmanned aerial vehicles (UAVs), which we will call Aerial Base Stations (ABSs), as shown in Figure 1. The use of such an ABS-based network offers an attractive solution to the problem of network under-utilization due to varying user density and provides the service provider with a significant reduction in CAPEX and OPEX.

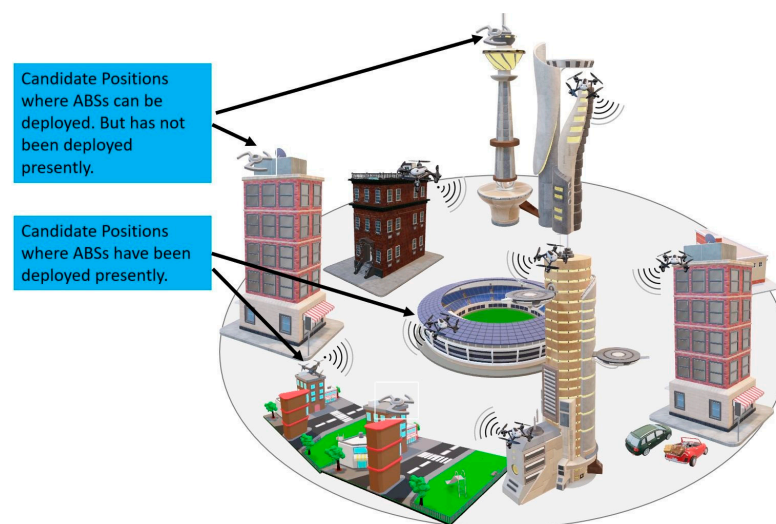


Figure 1. Aerial Base Station-based ultra-dense mobile network.

In the deployment of an ABS-based network, an immediate problem that arises is the optimal placement of the ABSs based on the user density distribution. Since UDNs are aimed at increasing capacity while ensuring the best user experience, such as providing higher data rates anywhere, therefore, for enhanced spectral efficiency, the received power and signal-to-interference ratio (SIR) should be higher. In this work, we study the problem of the optimal placement of ABSs at a subset of candidate locations that maximizes the total received power and the total SIR. A candidate position is a location where an ABS can be deployed and perched on a platform while it is deployed there. The deployed ABS can receive power at that location; so, when an ABS reaches its deployed candidate location, it does not need to hover. Furthermore, it means that there is no risk of a UAV or small cell running out of energy while it is operating at a candidate location. To the best of our knowledge, no other work has studied the problem of the optimal placement of ABSs at a set of discrete candidate locations as described above.

The main contributions of this work are as follows:

- This paper proposes a novel idea of potential candidate positions, a subset of which will be chosen for the placement of ABSs based on user density.

- This paper formulates the problem of optimal ABS placement at a subset of the candidate positions to maximize received power and SIR.
- This paper develops solutions for the formulated problems to determine the optimal placement of ABSs.

The rest of the paper is organized as follows. Section 2 gives a brief overview of related works. Section 3 describes the system model. In Section 4, the problem is formulated, whereas in Section 5, a solution for the problem is modeled in MATLAB. Section 6 discusses the simulation results and Section 7 draws some conclusions from this work.

2. Related Works

In recent years, researchers have been actively investigating the use of UAVs for providing communication services in a variety of scenarios, such as disaster-hit scenarios [4,5], extending coverage of fixed infrastructure [6], dealing with network overload conditions [7], etc. Moreover, the use of UAVs for enhancing the capabilities of the 5G network has also been investigated [8]. This work considers a UAV-based small cell network and investigates how ABSs can be optimally placed based on user density for improving received power and SIR.

The placement of ABSs affects various network performance parameters, such as coverage, throughput, connectivity, and revenue. The issue of mobile base station placement to maximize coverage is also studied in Wireless Sensor Networks (WSNs), where the goal is to place the base stations in a way that maximizes the number sensor nodes being covered, which resembles the problem of coverage maximization in mobile networks. There are works that attempt to maximize throughput or spectrum efficiency. In [9], the authors proposed an algorithm for optimizing the position of a single UAV for throughput maximization of users based on the user data rate requirements and their positions. In [4] the authors proposed an algorithm that determines optimal positions of multiple ABSs to maximize throughput considering a software-defined wireless network deployed in a disaster-hit area. In [10], the authors used deep learning to determine optimal UAV positions to maximize throughput. The authors of [11] studied maximizing the sum rate via power control and UAV positioning. Rosario et al. [12] studied the problem of UAV-based relays' placement to support high-quality live video transmission. In [13], the authors investigated the optimal altitude of low-altitude aerial platforms for coverage maximization.

Other works exploit the dynamic nature of UAV positioning to enhance network capacity. For example, considering a multi-tier drone-cell network to complement a terrestrial heterogeneous network, BorYaliniz et al. [14] studied the positioning of drone base stations (BSs) to maximize coverage and revenue. Guo et al. [15] conducted a theoretical analysis of how interference affects capacity and worked out a closed-form expression determining optimal ABS locations. Kalantari et al. [16] investigated the three-dimensional (3D) placement of ABSs to maximize the number of served users and their total rate. A mobility control algorithm has been proposed by Dixon et al. [17] for the optimal placement of a chain of UAV-based communication relays for enabling end-to-end communication. In [18], the authors investigated the optimum altitude for both static and mobile UAVs and its effects on the total power loss and bit error rates, etc. The authors of [19] propose an algorithm for the 3D placement of ABSs to maximize the coverage of users with different quality of service (QoS) requirements.

Since fixed-winged UAVs cannot hover at a particular location, there are works that attempt to enhance various network parameters through trajectory control of the UAVs. For example, Cheng et al. [20] proposed an iterative algorithm to determine optimal UAV trajectory for offloading traffic at the edge regions of three adjacent base stations. Zhan et al. [21] proposed an algorithm aimed at optimizing the performance of a ground-to-relay link by controlling the heading angle of the UAV. None of the solutions, and, to the best of our knowledge, any other related works, are suitable to efficiently solve the problem of receiving power and SIR maximization in ABS-based UDNs. Hence, this work studies this problem and designs a solution for it.

3. System Model

Let $U = \{1, 2, 3, \dots, N_u\}$ be the set of ABSs and $S = \{1, 2, 3, \dots, N_s\}$ be the set of users. Let $L = \{1, 2, 3, \dots, N_l\}$ be the set of N_l candidate locations for UAV placement. There are more candidate locations than the number of UAVs, i.e., $N_l > N_u$. All ABSs have the same transmission power P_s . We assume that the main source of noise for a user is the interference caused by ABSs other than the one with which the user is associated and that the thermal noise is negligible.

3.1. Aerial Base Stations

The small cells are mounted on UAVs called ABSs, and their deployment locations can be changed in response to user changes in density and mobility. We assume that the ABSs can autonomously move to the candidate location, perch, and connect to the power source there. Exactly how these tasks will be accomplished is outside the scope of this work, but given the rapid advancements in the autonomous flight of UAVs and localization, these assumptions are realistic.

3.2. Candidate Locations for ABSs

A candidate position is a location where an ABS can be deployed. We assume that each candidate position consists of a platform where an ABS can perch while it is deployed there and that the ABS can receive power at that location; so, when an ABS reaches its deployed candidate location, it does not need to hover. Furthermore, it means that there is no risk of a UAV or small cell running out of energy while it is operating at a candidate location. Furthermore, the batteries of a UAV can be charged while it is perched and operating at the candidate location. We assume that each candidate position has sufficient backhaul capacity to support the maximum possible traffic load generated at an ABS.

3.3. Path Loss Model

The air-to-ground path loss model [13,22] is used, which gives, in a probabilistic manner, the average path loss:

$$PL(dB) = 20 \log \frac{4\pi f_c d}{c} + P(NLoS) \eta_{NLoS} \quad (1)$$

where d is the distance between the ABS and receiver, $P(LoS)$ is the line-of-sight (LoS) probability, and $P(NLoS)$ is the non-line-of-sight probability. Furthermore, η_{LoS} and η_{NLoS} represent the additional losses in the cases of LoS and NLoS, respectively. The value for d is given by $\sqrt{h^2 + r^2}$, where h and r are the altitudes of the UAV and its horizontal distance from the receiver, respectively. $P(LoS)$ is given by

$$P(LoS) = \frac{1}{1 + a \exp(-b(\theta - a))} \quad (2)$$

where a and b are constants depending on the environment and θ is the elevation angle (in degrees) given by $\frac{180}{\pi} \arctan\left(\frac{h}{r}\right)$. $P(NLoS) = 1 - P(LoS)$.

4. Problem Formulation

Let A_i be a zero–one indicator variable with $A_i = 1$ if an ABS is deployed at candidate location i ; otherwise, $A_i = 0$. Similarly, let $B_{i,j}$ be a zero–one indicator variable with $B_{i,j} = 1$ if user j is connected to the ABS at candidate location i ; otherwise, $B_{i,j} = 0$. Let $P_{i,j}$ be the power received by user j from the ABS at location i . If user j is connected to the ABS at location r , then the signal-to-interference noise ratio at user j will be:

$$SIR_j = \frac{P_{r,j}}{\sum_{i \in L, i \neq r} P_{i,j}} \quad (3)$$

The goal is to place the ABSs in candidate locations and to assign users to ABSs to maximize the sum of SIR for all users, that is,

$$\underset{A_i, B_{i,j}, \forall i \in L, \forall j \in S}{\text{maximize}} \sum_{j \in S} \text{SIR}_j \quad (4)$$

If all the ABSs use different frequency bands, then the goal will be to maximize the sum of received powers (i.e., received signal strength (RSSI)). Let P_j be the power received by a user j from the candidate location to which it is assigned; then,

$$\underset{A_i, B_{i,j}, \forall i \in L, \forall j \in S}{\text{maximize}} \sum_{j \in S} P_j \quad (5)$$

In Equations (4) and (5), A_i controls where to place an ABS and $B_{i,j}$ controls to which location to assign a user such that the corresponding summation is maximized.

A user j can only be assigned to a candidate location i if there is an ABS placed at that candidate location, i.e., $A_i = 1$. This means:

$$A_i B_{i,j} = 1, \forall j \in S \quad (6)$$

A user should be assigned to exactly one candidate location, which means:

$$\sum_{i \in L} B_{i,j} = 1, \forall j \in S \quad (7)$$

As N_u is the number of ABSs, the following constraint should be satisfied:

$$\sum_{i \in L} A_i = N_u \quad (8)$$

4.1. Maximizing the Sum of Received Powers

The problem of maximizing the sum of powers is formally defined below.

$$\underset{A_i, B_{i,j}, \forall i \in L, \forall j \in S}{\text{maximize}} \sum_{j \in S} P_j \quad (9a)$$

$$\text{subject to: } A_i B_{i,j} = 1, \forall j \in S \quad (9b)$$

$$\sum_{i \in L} B_{i,j} \quad (9c)$$

$$\sum_{i \in L} A_i \quad (9d)$$

4.2. Maximizing the Sum of SIRs

The problem of maximizing the sum of SIRs is formally defined below.

$$\underset{A_i, B_{i,j}, \forall i \in L, \forall j \in S}{\text{maximize}} \sum_{j \in S} \text{SIR}_j \quad (10a)$$

$$\text{subject to: } A_i B_{i,j} = 1, \forall j \in S \quad (10b)$$

$$\sum_{i \in L} B_{i,j} \quad (10c)$$

$$\sum_{i \in L} A_i \quad (10d)$$

5. Solution Modeling

The optimization problems posed in Sections 4.1 and 4.2 are 0–1 integer programming problems and computationally fall in the class of NP-complete problems. We used MATLAB's bintprog to solve these problems.

The function $[X \text{ Val}] = \text{bintprog}(F, A, B, A_{\text{eq}}, B_{\text{eq}})$ produces a vector X whose entries are binary values and a variable $\text{Val} = F^T X$, which is the value that is minimized; F^T represents the transpose of F . The arguments A_{eq} and B_{eq} are used for equality constraints such that $A_{\text{eq}}X = B_{\text{eq}}$, whereas A and B are used for inequality constraints such that $AX \leq B$. A_{eq} is a matrix whose number of rows should equal the number of equality constraints and whose columns should equal to the number of 0–1 variables.

Based on the positions of users and candidate locations, applicable channel model, transmission power, etc., for each user, the RSSI from each candidate position is calculated and stored in an N_s -by- N_l matrix P , where $P_{i,j}$ represents the power received by user i from candidate location j .

For our problem of received power maximization defined in Section 4.1, A_{eq} is an $(N_s + 1)$ -by- $(N_s + 1)N_l$ matrix, whereas B_{eq} is an $(N_s + 1)$ -by-1 vector. This means that there are $N_s + 1$ equality constraints. The first equality constraint ensures that exactly N_u UAVs (small cells) are deployed and the remaining N_s constraints ensure that each user is assigned to exactly one candidate location. (Note that we ensure through inequality constraints that each user is assigned to a candidate location with a deployed small cell; we will discuss this shortly). F is an $(N_s + 1)N_l$ -by-1 vector and is constructed such that the first N_l entries are set to zero and entries $iN_l + 1$ through $(i + 1)N_l$ are set to the received powers of user i from all candidate locations: 1 through N_l . A_{eq} is constructed as given in Algorithm 1.

Algorithm 1: Construction of matrix A_{eq} for received power maximization

Input: Number of users, N_s and Number of candidate positions, N_l

Output: Matrix A_{eq}

```

for  $i = 1$  upto  $N_s + 1$ 
     $A_{\text{eq}}[i][(i - 1)N_l + 1:(i - 1)N_l + N_l] = 1$ 
end

```

The vector B_{eq} is constructed as $B_{\text{eq}} = [N_u \ O]^T$, where N_u is the number of ABSs and O is row vector of size N_s and each of its entries is 1. Moreover, A is an $N_s N_l$ by $(N_s + 1)N_l$ matrix, whereas b is an $N_s N_l$ -by-1 vector. Then, for the inequality constraint, the matrix is constructed as given in Algorithm 2.

Algorithm 2: Construction of matrix A for received power maximization

Input: Number of users, N_s and Number of candidate positions, N_l

Output: Matrix A

```

for  $i = 1$  upto  $N_s$ 
    for  $j = 1$  upto  $N_l$ 
         $A[(i - 1)N_l + j][j] = 1$ 
         $A[(i - 1)N_l + j][iN_l + j] = -1$ 
    end
end

```

B is an $N_s N_l$ -by-1 column vector and is initialized to all zero entries; that is, $B[1:N_s N_l] = 0$. The matrix F is constructed as shown in Algorithm 3.

Algorithm 3: Construction of vector F for received power maximization

Input: Number of users, N_s , Number of candidate positions, N_l and Matrix of received powers, P
Output: Vector F

```

F[1: $N_l$ ] = 0
for  $i = 1$  upto  $N_s$ 
    F[ $iN_s + 1 : (i + 1)N_s$ ] = P[ $i$ ][:]
end
F = FT

```

For the problem of SIR optimization defined in Section 4.2, matrix A_{eq} is constructed as given in Algorithm 4.

Algorithm 4: Construction of matrix A_{eq} for SIR maximization

Input: Number of users, N_s and Number of candidate positions, N_l
Output: Matrix A_{eq}

```

Take two auxiliary matrices T and Z, each of dimensions  $(N_s + 1)$ -by- $(N_s N_l + N_l)$  of all zero entries
for  $i = 1$  upto  $N_s + 1$ 
    T[ $i$ ][ $(i - 1)N_l + 1 : (i - 1)N_l + N_l$ ] = 1
end
 $A_{eq} = \begin{bmatrix} T & Z \\ Z & T \end{bmatrix}$ 
 $A_{eq}[1][N_l + 1 : 2(N_s N_l + N_l)] = 0$ 

```

Then, B_{eq} is constructed as $B_{eq} = [N_u \ O \ N_u \ (N_u - 1)O]^T$, where O is a row vector of size N_s containing all ones.

The inequality constraint matrices A for SIR maximization is constructed as shown in Algorithm 5.

Algorithm 5: Construction of matrix A for SIR maximization

Input: Number of users, N_s and Number of candidate positions, N_l
Output: Matrix A

```

Take four auxiliary amtrices  $A_1, A_2, A_3$  and  $A_4$  each of dimensions  $N_s N_l$ -by- $(N_s + 1)N_l$  Initialize
 $A_1, A_2, A_3$  and  $A_4$  to zero (that is, make all their entries zero)
for  $i = 1$  upto  $N_s$ 
    for  $j = 1$  upto  $N_l$ 
         $A_1[(i - 1)N_l + j][j] = 1$ 
         $A_1[(i - 1)N_l + j][iN_l + j] = -1$ 
         $A_2[(i - 1)N_l + j][j] = 1$ 
         $A_3[(i - 1)N_l + j][iN_l + j] = -1$ 
    end
end
 $A = \begin{bmatrix} A_1 & A_4 \\ A_2 & A_3 \end{bmatrix}$ 

```

B is a $(2N_s N_l + N_l)$ -by-1 column vector and is initialized to all zero entries.

The matrix F is then constructed as given in Algorithm 6.

Figure 2 shows the flowchart of the designed solutions. The flowchart first checks whether the received power or the SIR needs to be maximized. Once this choice is made, the matrices and vectors needed for the bintprog as input are constructed in a series of steps. As described above, this construction ensures that all constraints, as specified in the problem formulation, are satisfied. As evident from the discussion above and from the flowchart, the construction processes for each problem is different from the other and involves using matrices and vectors of certain dimensions and then filling out certain

entries in those matrices and vectors, thereby incorporating the problem constraints and ensuring, for each problem, that the bintprog properly evaluates the objective function.

Algorithm 6: Construction of vector F for received power maximization

Input: Number of users, N_s , Number of candidate positions, N_l and Matrix of received powers, P

Output: Vector F

$F_1[1:N_l] = 0;$

for $i = 1$ **upto** N_s

$F_1[iN_s + 1 : (i + 1)N_s] = P[i][:]$

$F_1 = F_1^T$

$F = \begin{bmatrix} F_1 \\ -F_1 \end{bmatrix}$

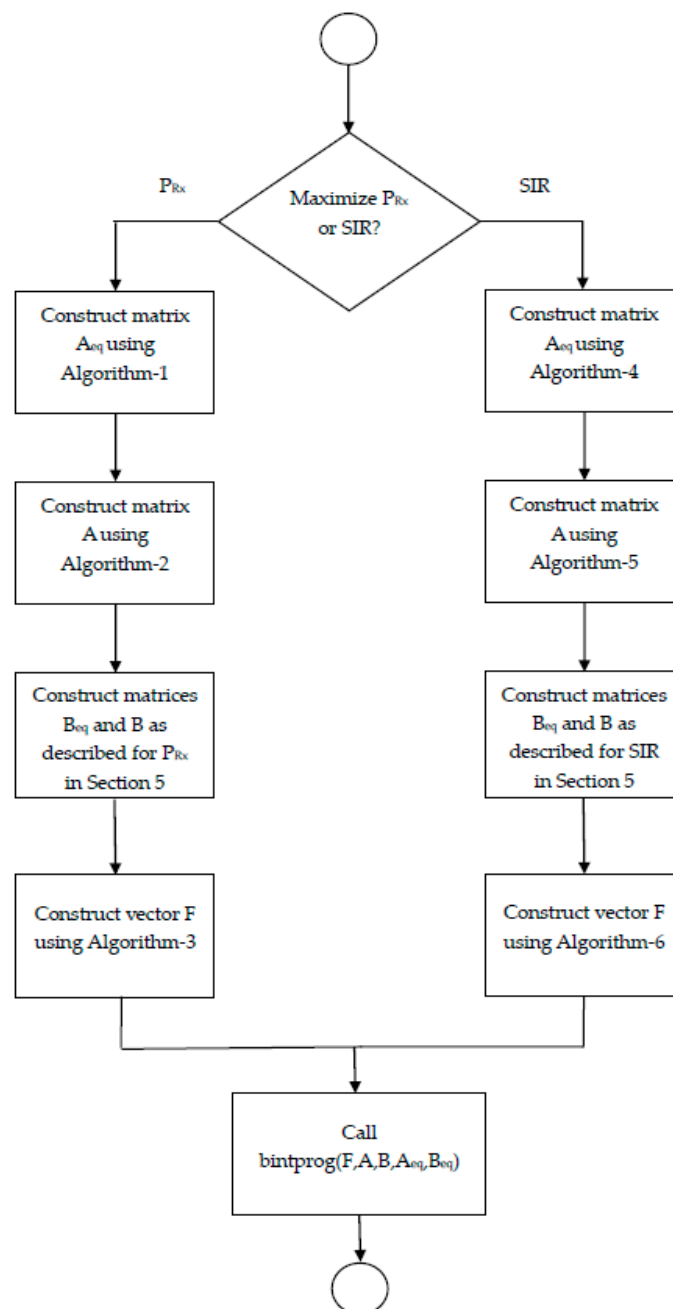


Figure 2. Flowchart indicating the steps the proposed solutions involve.

6. Results and Discussion

In this section, we discuss the MATLAB simulation results obtained while studying the effect of various parameters on performance improvement due to the optimal placement of the Aerial BSs.

The deployment area was kept at $1000 \times 1000 \text{ m}^2$. The heights of candidate positions (and hence those of the ABSs) were maintained between 50 and 100 m. The transmit power of the ABSs was kept at 30 dBm. User positions were generated using the Poisson point process and Poisson cluster process. A Poisson cluster process is a mathematical model used to describe the spatial distribution of points in a given region. In this process, points are grouped into clusters, where each cluster is generated independently according to a Poisson distribution. The superposition of these clusters allows for individual points to be random and have the tendency to cluster together in certain regions. Candidate positions for ABSs were generated using evenly spaced grid points. A suburban environment was considered with the parameters given in Table 1.

Table 1. Parameters for the suburban environment.

Parameter	Value
a	4.88
b	0.49
η_{LoS}	0.1 dB
η_{NLoS}	21 dB

6.1. Results

Figure 3 demonstrates how the dynamic repositioning of BSs enhances performance. In particular, the figure shows how the optimal placement of the ABSs becomes suboptimal due to the mobility of users. With the passage of time, the suboptimality increases and, hence, the normalized total received power decreases. After a time of 100 epochs, the optimal positions for the ABSs are recomputed, and the ABSs are repositioned, which results again in the maximum achievable total received power. Note that the vertical scale has been normalized between 0 and 1 by subtracting the minimum value from the data and then dividing it by the maximum value.

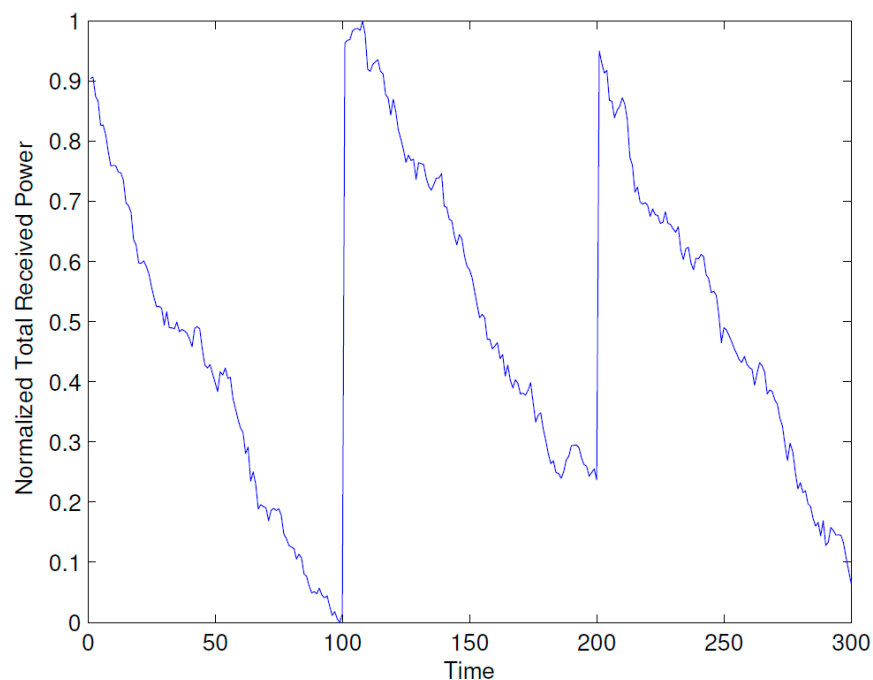


Figure 3. Degradation in total received power due to mobility of users.

Figure 4 shows the effect of the number of ABSs on the improvement in the total received power that is achieved with the optimal placement of the ABSs compared to a uniform distributed placement. The user positions were created using two different deployment processes: the Poisson cluster process and the Poisson process. In the Poisson cluster process, users tend to concentrate around certain hot spots. The candidate positions of the ABSs were created using squared grids of 5-by-5, 6-by-6, and 7-by-6. From Figure 4, it is evident that greater improvement in the total received power is achieved with the optimal placement of the ABSs compared to the Poisson cluster process. Moreover, it is evident from the figure that by increasing the grid resolution (number of candidate positions), greater improvement in the total received power is achieved. Furthermore, it can also be observed that maximum improvement is achieved when the number of ABSs is equal to the square root of the grid dimensions: that is N , for a grid of N -by- N maximum improvement is achieved when the number of ABSs is N .

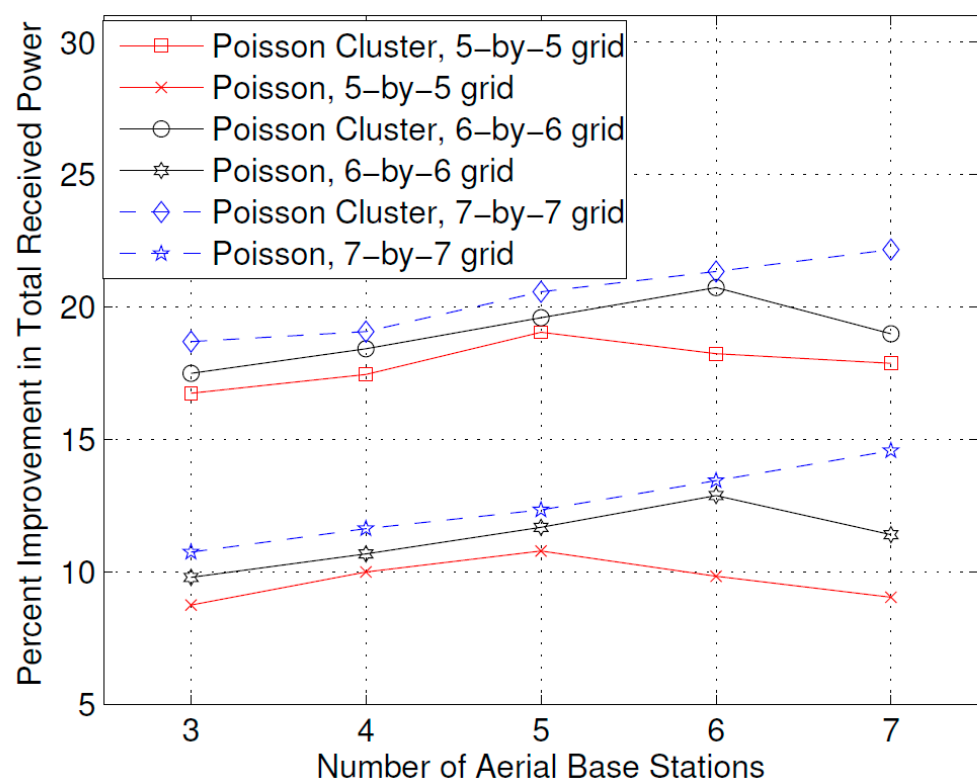


Figure 4. Percent improvement in received power with respect to the number of Aerial BSs.

Figures 5 and 6 show the probability mass function (PMF) of the percentage of users receiving improvement in their received power due to the optimal placement of the ABSs for the Poisson cluster process and Poisson process of user position generation, respectively, whereas Figure 7 shows their cumulative probability distribution function (CCDF). From these figures, it is evident that in the Poisson cluster process, there is more than a 0.8 probability for 60 percent or more users to receive improvement because of optimal placement of ABSs and more than a 0.5 probability for 80 percent or more users. Similarly, for the Poisson process, there is more than a 0.8 probability for 40 percent or more users to receive improvement due to the optimal ABS placements and an approximately 0.4 probability for 60 percent or more users.

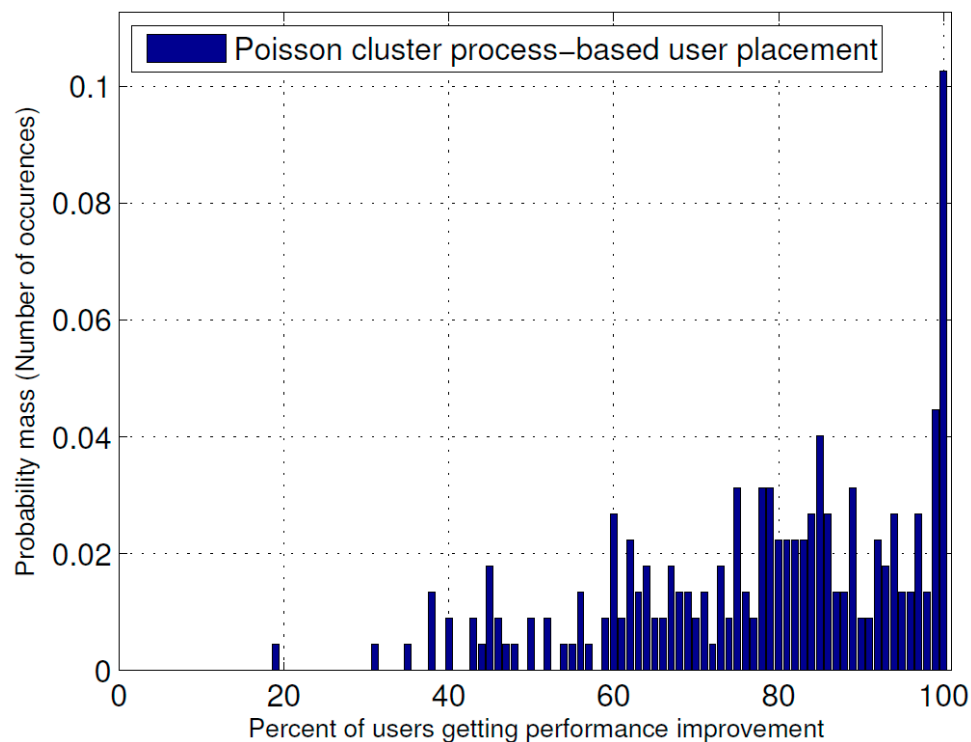


Figure 5. PMF of the percentage of users receiving performance improvement when user positions were generated as Poisson cluster process.

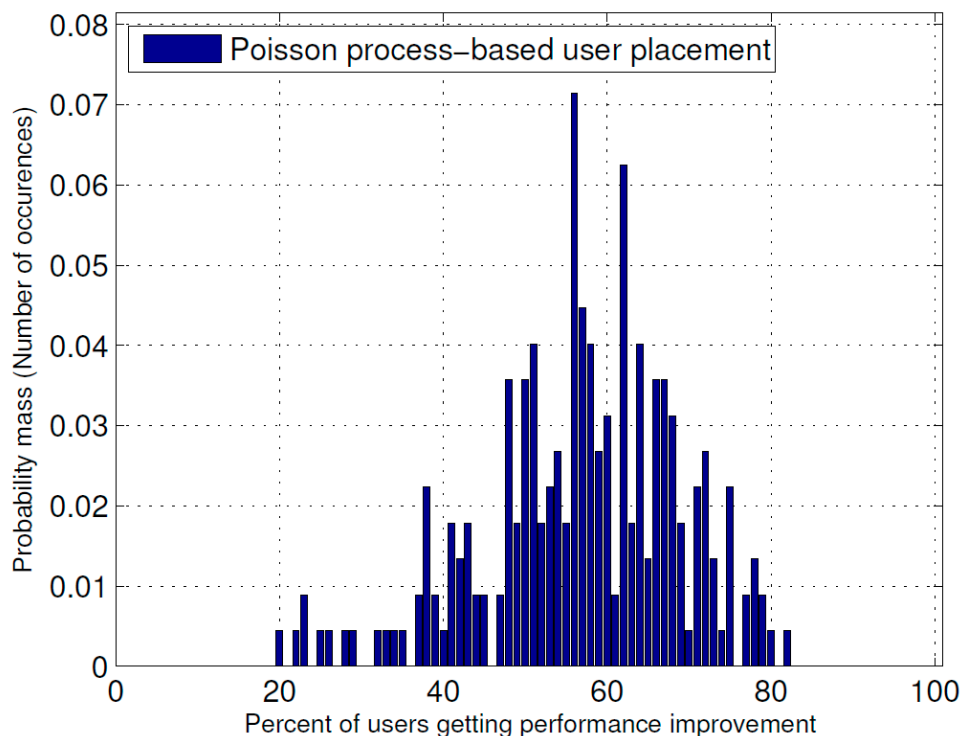


Figure 6. PMF of the percentage of users receiving performance improvement when user positions were generated as Poisson point process.

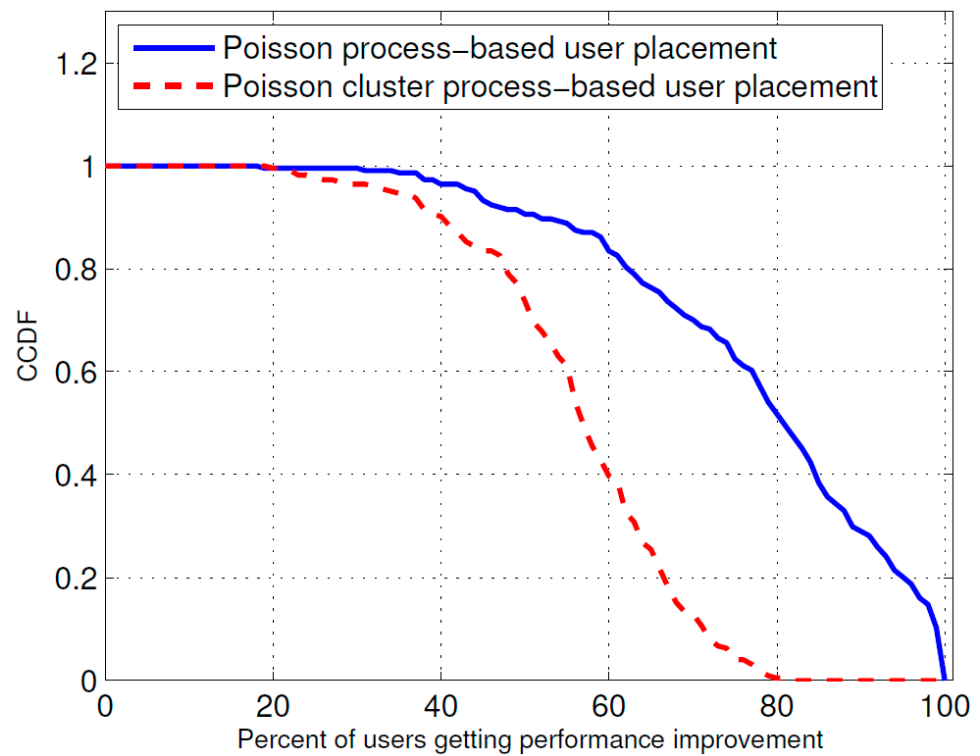


Figure 7. CCDF for percentage of users receiving performance improvement.

Figure 8 shows the effect of the number of candidate positions on the improvement in received power due to the optimal placement of the ABSs. Increasing the number of candidate positions results in more improvement in the received power. This can be explained by the fact that with more candidate positions, there are more suitable positions for placing the Aerial BSs compared to fewer candidate positions.

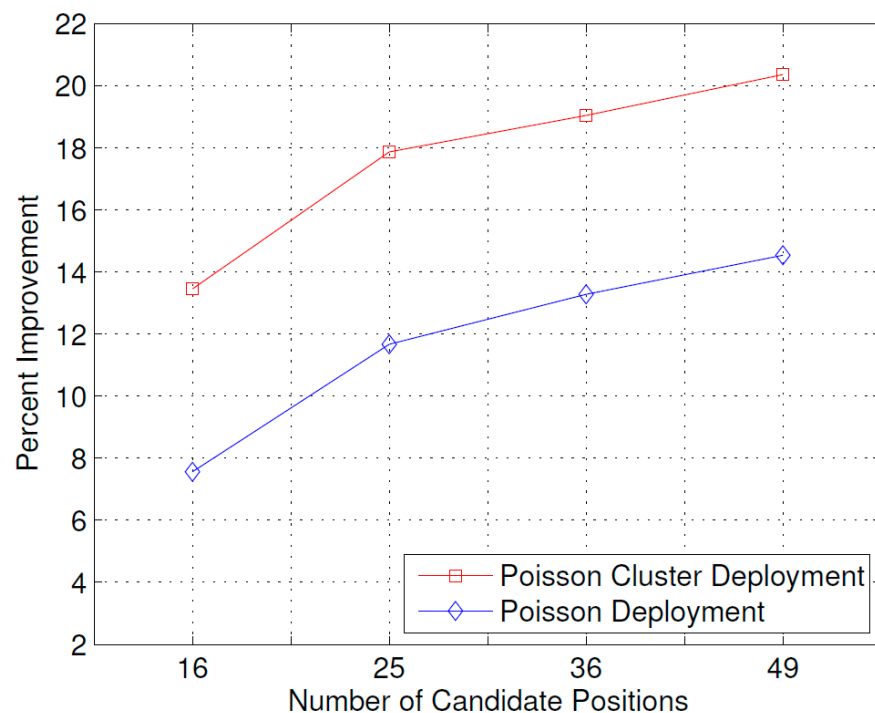


Figure 8. Effect of the number of candidate positions on improvement in received power.

Figure 9 shows the effect of the number of ABSs on the improvement in the SIR obtained due to optimal placement of the ABSs. It is interesting to note that, unlike the case for received power, as shown in Figure 4, the increase in the number of ABSs leads to a decrease in percent improvement in the SIR. This may be explained by the fact that when the number of ABSs increases, the amount of interference that a user receives also increases, as concluded by some stochastic geometry studies of UDNs [23]; therefore, although the optimal placement still achieves an improvement in the SIR, this improvement is lower compared to the case when there are fewer ABSs. To reduce the effects of increased interference due to the increase in the number of ABSs, one solution can be to assign different channels to neighboring ABSs or use beamforming techniques [24,25]. Channel allocation and beamforming are, however, out of the scope of this work.

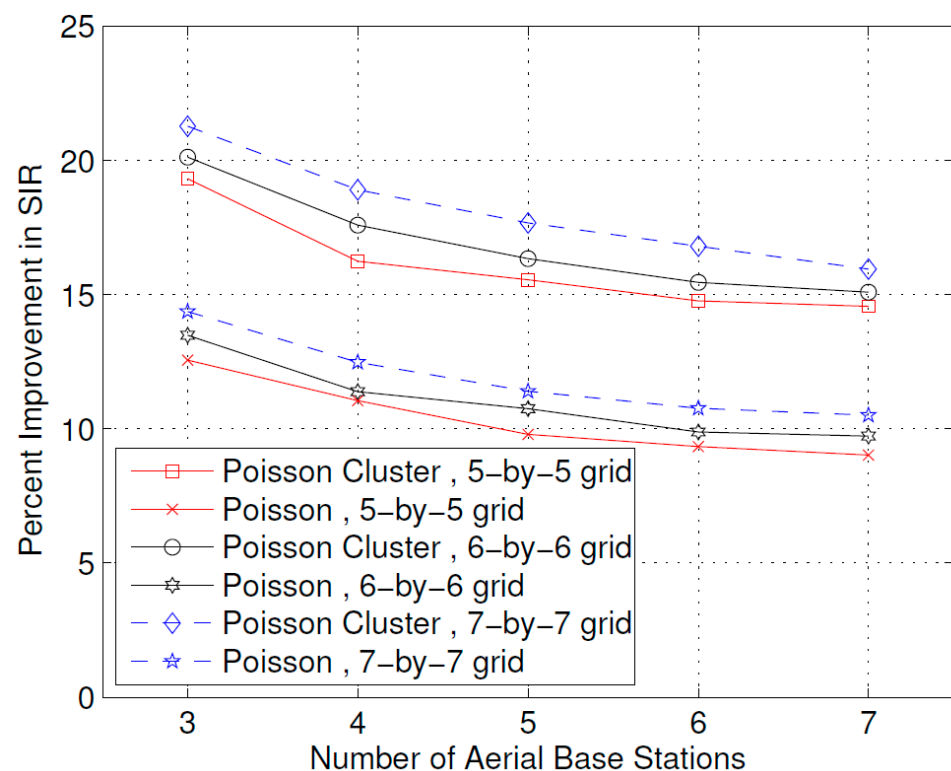


Figure 9. Percent improvement in SIR with respect to number of Aerial BSs.

Figure 10, just like the case for total received power shown in Figure 8, shows the effect of the number of candidate positions on the improvement in SIR achieved by the optimal placement of the ABSs. As the number of candidate positions increases, the improvement in the received SIR also increases for both user distribution types; however, the rate of increase, in this case, is lower compared to that of the total received power, as shown in Figure 8. The same reasons given in explanation of the results of Figure 9 may be attributed to this observation.

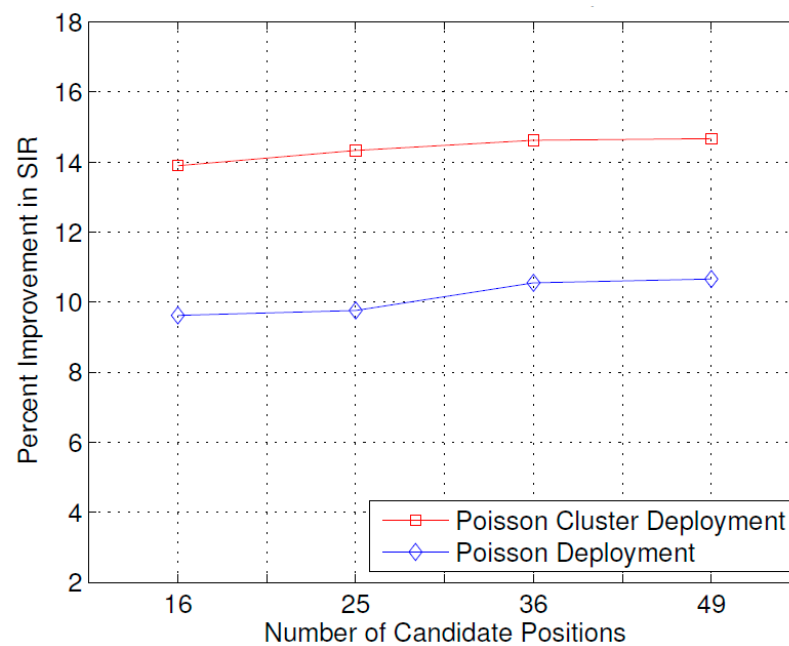


Figure 10. Effect of the number of candidate positions on improvement in SIR.

6.2. Discussion

The results presented above support the idea that the dynamic repositioning of ABSs based on user densities can significantly enhance user experience. For Example, Figure 3 shows that when ABSs are placed at optimal candidate positions, users' received power is higher, but with the passage of time and user mobility, that placement becomes suboptimal. Therefore, the need for recomputing the optimal positions arises again, and when that is complete and the ABSs are moved to the newly computed optimal candidate positions, the users' received power significantly increases. Evidently, this dynamic repositioning would not be possible without the use of ABSs, or any other aerial platform that could carry the transmission equipment and move to a target location. Figure 4 shows that depending on the arrangement of the candidate positions, increasing the number of ABSs to a certain limit results in a greater increase in the received power; however, that improvement starts to fall beyond that optimal number of ABSs, which, in the produced results, appears to be the square root of the number of candidate positions. Figures 4–6 together indicate that a significant number of users benefit from the dynamic repositioning of ABSs in the form of improved received power and improved SIR. The percentage of users receiving improved received power is higher than the percentage of users receiving improved SIR. This indicates that if neighboring ABSs are allotted different channels, the performance improvement will be greater. Figure 8 shows that increasing the number of candidate positions leads to more improvement in the percentage improvement in the received power. This is because with more candidate positions, there is more flexibility in the placement of the ABSs, which aligns better with the benefits associated with the dynamic placement of ABSs. Figure 9 shows that increasing the number of ABSs leads to more interference and hence less improvement in SIR, which is consistent with other studies on the impact of the number of base stations on the SIR such as [23]. Figure 10 shows that increasing the number of candidate positions leads to greater improvement in the SIR; however, the rate of increase is smaller compared to that of received power, as shown in Figure 8. The overall observation is that the dynamic placement of ABSs has the potential for improving user experience and that the greater the number of candidate positions, the higher the improvement. Moreover, allocating different channels to neighboring ABSs leads to more improvement in performance with dynamic placement.

7. Conclusions and Future Work

A novel idea for the dynamic placement (repositioning) of small cells based on user locations and concentrations was proposed. The problem was formally formulated, and an optimization solution was designed and implemented in MATLAB. The effect of various parameters was studied on the improvement in received power and SIR. The results showed that by increasing the number of Aerial BSs, a greater increase in received power can be achieved. Similarly, increasing the number of candidate positions also leads to a greater increase in received power and SIR. Furthermore, when the user positions are more concentrated in hot spots, the optimal placement results in significantly more improvement in the received power and SIR, which range between 16 and 22 percent and 13 and 21 percent, respectively. When the user positions are distributed as the Poisson point process, the improvement in received power ranges between 8 and 15 percent and 7 and 15 percent, respectively. This work studied the improvement in received power and SIR due to the dynamic placement, and in future work, other aspects of dynamic placement may be studied. For example, a future extension of this work might be to study the joint optimization of ABS placement and channel allocation. Another possible extension might be the joint capacity enhancement and user experience optimization.

Author Contributions: S.U.R. proposed the idea, performed simulations, and wrote the technical section of the paper. A.K. wrote the introduction and related work, and drew the figures in the manuscript. M.U. helped to gather different parameters related to simulations. M.B. proofread this work. Y.-Z.C. helped in Funding acquisition and review. H.E.-S. Provided computation resources. All authors have read and agreed to the published version of the manuscript.

Funding: This research was supported in part by the Basic Science Research Program through the National Research Foundation of Korea (NRF) funded by the Ministry of Education (No. NRF-2018R1A6A1A03025109) and by the National Research Foundation of Korea (NRF) grant funded by the Korea government (MSIT) (No. 2023R1A2C1003928).

Institutional Review Board Statement: Not applicable.

Informed Consent Statement: Not applicable.

Data Availability Statement: Not applicable.

Acknowledgments: This research was supported in part by the Basic Science Research Program through the National Research Foundation of Korea (NRF) funded by the Ministry of Education (No. NRF-2018R1A6A1A03025109) and by the National Research Foundation of Korea (NRF) grant funded by the Korea government (MSIT) (No. 2023R1A2C1003928).

Conflicts of Interest: The authors declare no conflict of interest.

References

1. Harald, B.; Blennerud, G.; Burststedt, F.; Chaisatien, W.; Karikyt, M. *Ericsson Mobility Report*; Tech. Rep.: Stockholm, Sweden, 2022.
2. Andrews, J.G.; Buzzi, S.; Choi, W.; Hanly, S.V.; Lozano, A. What will 5g be? *IEEE J. Sel. Areas Commun.* **2014**, *32*, 1065–1082. [[CrossRef](#)]
3. Khodabandelou, G.; Gauthier, V.; Fiore, M.; El-Yacoubi, M.A. Estimation of static and dynamic urban populations with mobile network metadata. *IEEE Trans. Mob. Comput.* **2019**, *18*, 2034–2047. [[CrossRef](#)]
4. Rahman, S.U.; Kim, G.-H.; Cho, Y.-Z.; Khan, A. Positioning of UAVs for throughput maximization in software-defined disaster UAV communication networks. *J. Commun. Netw.* **2018**, *20*, 452–463. [[CrossRef](#)]
5. Liu, X.; Li, Z.; Zhao, N.; Meng, W.; Gui, G. Transceiver design and multihop d2d for UAV IoT coverage in disasters. *IEEE Internet Things J.* **2019**, *6*, 1803–1815. [[CrossRef](#)]
6. Horváth, D.; Gazda, J.; Šlapak, E.; Maksymyuk, T.; Dohler, M. Evolutionary coverage optimization for a self-organizing UAV-based wireless communication system. *IEEE Access* **2021**, *9*, 145066–145082. [[CrossRef](#)]
7. Zhang, Q.; Saad, W.; Bennis, M.; Lu, X.; Debbah, M. Predictive deployment of UAV base stations in wireless networks: Machine learning meets contract theory. *IEEE Trans. Wirel. Commun.* **2021**, *20*, 637–652. [[CrossRef](#)]
8. Zeng, Y.; Guvenc, I.; Zhang, R.; Geraci, G.; Matolak, D. *UAV Communications for 5G and Beyond*; John Wiley and Sons Inc.: Hoboken, NJ, USA, 2020.
9. Rahman, S.U.; Cho, Y.Z. UAV positioning for throughput maximization. *EURASIP J. Wirel. Commun. Netw.* **2018**, *2018*, 31. [[CrossRef](#)]

10. Munaye, Y.Y.; Lin, H.-P.; Adege, A.B.; Tarekegn, G.B. UAV positioning for throughput maximization using deep learning approaches. *Sensors* **2019**, *19*, 2775. [[CrossRef](#)] [[PubMed](#)]
11. Li, L.; Chang, T.-H.; Cai, S. UAV positioning and power control for two-way wireless relaying. *IEEE Trans. Wirel. Commun.* **2020**, *19*, 1008–1024. [[CrossRef](#)]
12. Rosário, D.; Filho, J.A.; do Rosário, D.; Santos, A.; Gerla, M.L. A relay placement mechanism based on UAV mobility for satisfactory video transmissions. In Proceedings of the 16th Annual Mediterranean Ad Hoc Networking Workshop, Med-Hoc-Net, Budva, Montenegro, 28 June 2017.
13. Al-Hourani, A.; Kandeepan, S.; Lardner, S. Optimal lap altitude for maximum coverage. *IEEE Wirel. Commun. Lett.* **2014**, *3*, 569–572. [[CrossRef](#)]
14. Bor-Yaliniz, I.; Yanikomeroglu, H. The new frontier in ran heterogeneity: Multi-tier drone-cells. *Comm. Mag.* **2016**, *54*, 48–55. [[CrossRef](#)]
15. Guo, W.; and Farrell, T.O. Relay deployment in cellular networks: Planning and optimization. *IEEE J. Sel. Areas Commun.* **2013**, *31*, 1597–1606.
16. Kalantari, E.; Shakir, M.Z.; Yanikomeroglu, H.; Yongaçoglu, A. Backhaul-aware robust 3D drone placement in 5G+ wireless networks. *arXiv* **2017**, arXiv:1702.08395.
17. Dixon, C.; Frew, E.W. Optimizing cascaded chains of unmanned aircraft acting as communication relays. *IEEE J. Sel. Areas Commun.* **2012**, *30*, 883–898. [[CrossRef](#)]
18. Chen, Y.; Feng, W.; Zheng, G. Optimum placement of UAVs as relays. *IEEE Commun. Lett.* **2018**, *22*, 248–251. [[CrossRef](#)]
19. Alzenad, M.; El-Keyi, A.; Yanikomeroglu, H. 3-d placement of an unmanned aerial vehicle base station for maximum coverage of users with different QoS requirements. *IEEE Wirel. Commun. Lett.* **2018**, *7*, 38–41. [[CrossRef](#)]
20. Cheng, F.; Zhang, S.; Li, Z.; Chen, Y.; Zhao, N. UAV trajectory optimization for data offloading at the edge of multiple cells. *IEEE Trans. Veh. Technol.* **2018**, *67*, 6732–6736. [[CrossRef](#)]
21. Zhan, P.; Yu, K.; Swindlehurst, A.L. Wireless relay communications with unmanned aerial vehicles: Performance and optimization. *IEEE Trans. Aerosp. Electron. Syst.* **2011**, *47*, 2068–2085. [[CrossRef](#)]
22. Al-Hourani, A.; Kandeepan, S.; Jamalipour, A. Modeling air-toground path loss for low altitude platforms in urban environments. In Proceedings of the IEEE Global Communications Conference, Austin, TX, USA, 8 December 2014.
23. Filo, M.; Foh, C.H.; Vahid, S.; Tafazolli, R. Performance impact of antenna height in ultra-dense cellular networks. In Proceedings of the IEEE International Conference on Communications Workshops (ICC Workshops), Paris, France, 3 July 2017.
24. Lin, Z.; Lin, M.; Champagne, B.; Zhu, W.-P. Secrecy-Energy Efficient Hybrid Beamforming for Satellite-Terrestrial Integrated Networks. *IEEE Trans. Commun.* **2021**, *69*, 6345–6360. [[CrossRef](#)]
25. Lin, Z.; An, K.; Niu, H.; Hu, Y.; Chatzinotas, S.; Zheng, G.; Wang, J. SLNR-Based Secure Energy Efficient Beamforming in Multibeam Satellite Systems. *IEEE Trans. Aerosp. Electron. Syst.* **2023**, *59*, 2085–2088. [[CrossRef](#)]

Disclaimer/Publisher’s Note: The statements, opinions and data contained in all publications are solely those of the individual author(s) and contributor(s) and not of MDPI and/or the editor(s). MDPI and/or the editor(s) disclaim responsibility for any injury to people or property resulting from any ideas, methods, instructions or products referred to in the content.